available at www.sciencedirect.com

SCIENCE DIRECT®

journal homepage: www.elsevier.com/locate/biochempharm

Schisandrin B enhances doxorubicin-induced apoptosis of cancer cells but not normal cells

Ling Li, Qinghua Lu, Yanwei Shen, Xun Hu *

The Cancer Institute, The Second Affiliated Hospital, Zhejiang University School of Medicine, 88 Jiefang Road, Hangzhou, PR China

ARTICLE INFO

Article history:
Received 19 August 2005
Accepted 28 November 2005

Keywords:
Apoptosis
Doxorubicin
Schisandrin B
Caspase
Cardiomyocytes

Abbreviations:
Sch B, Schisandrin B
DOX, doxorubicin
MDR, multidrug resistance
P-gp, P-glycoprotein
MRP1, multidrug resistance related protein 1
FACS, fluorescence-activated cell sorting
MTT, 3-(4,5-dimethylthiazole-2yl)-2,5-diphenyl tetrazolium bromide
RT-PCR, reverse transcription-PCR
PARP, poly(ADP-ribose) polymerase
MMP, mitochondria membrane potential

ABSTRACT

The dose-dependent cardiotoxicities of doxorubicin (DOX) significantly limits its anti-cancer efficacies. One of the ways to augment the efficacies of DOX at a relatively low cumulative dose is to use a chemical sensitizer. Here, we demonstrated that schisandrin B (Sch B) significantly enhanced DOX-induced apoptosis of SMMC7721, a human hepatic carcinoma cell line, and of MCF-7, a human breast cancer cell line. This enhancement was irrelevant to the action of Sch B on P-glycoprotein or other drug-transporters, but associated with the activation of caspase-9 rather than caspase-8. The loss of mitochondria membrane potential was observed when cells were treated with DOX and Sch B combined. On the other hand, at the same experimental conditions, Sch B did not enhance the DOX-induced apoptosis of primary rat cardiomyocytes and primary human fibroblasts. Therefore, it is speculative that Sch B may bring benefit to clinical chemotherapy by reducing significantly the cumulative doses of DOX and its associated cardiotoxicities.

* *Corresponding author*. Tel.: +86 571 87783656
E-mail address: huxun@zju.edu.cn (X. Hu).

0006-2952/$ – see front matter
doi:10.1016/j.bcp.2005.11.026

1. Introduction

The successful treatment of cancer involving DOX is limited to a significant extent by its cardiotoxicities [1]. Once the cumulative dose reaches 500 mg/m^2, further increment of DOX would drastically increase the cardiomyopathy and congestive heart failure. Therefore, to increase the potency of DOX at the doses with clinically acceptable adverse effects is one of the determinants for the successful chemotherapy.

The anti-cancer efficacies of DOX rely on its potency to induce the apoptosis of cancer cells. Two distinct apoptotic signaling pathways have been described. The first signaling pathway is triggered by the death receptors (i.e. CD95/Apo-1/Fas or TRAIL), the members of the tumor necrosis factor receptor family [2–4]. After activation of these receptors, caspase-8 is cleaved, followed by the activation of the downstream effector caspases-3, -6 and -7. The second apoptosis pathway is signaled by the cytosolic release of cytochrome *c* from the mitochondria, which then initiates the formation of apoptosome (APAF1/cytochrome *c*/pro-caspase-9 complex), where pro-caspase-9 is autocleaved to its active form. Caspase-9 then primed the execution phase of apoptosis. It has been well documented that DOX is able to induce apoptosis via mitochondrial pathway [5,6], although it is still controversial if death receptor pathway is a major mechanism of DOX-induced apoptosis [7–9]. On the other hand, cancer cells could develop many mechanisms to reduce the anti-cancer efficacies of DOX, such as expression of the MDR1 gene [10], production of some apoptotic inhibitors such as Bcl-2 or IAP3, and HSP70 [11,12], etc.

One of the ways to increase the efficacies of anti-cancer drug is to use a sensitizer, which itself does not have the activities to kill cancer cells, but can significantly enhance the potency of the anti-cancer drugs [12–14]. Schisandrin B (Fig. 1), the most abundant dibenzocyclooctadiene lingnan isolated from the traditional Chinese medicinal herb *Schisandra chinensis* (Turcz.) *Baill*, was shown to protect against carbon tetrachloride-induced liver damage and myocardial ischemia-reperfusion injury through removal of ROS via enhanced cellular glutathione antioxidant status [15]. Recently, we reported that this compound was a novel inhibitor of P-glyocoprotein (P-gp) [16]. In this study, we demonstrated that Sch B could significantly enhance the DOX-induced apoptosis of SMMC7721, a human hepatic cancer cell line, and MCF-7, a human breast cancer cell line, through a mechanism associated with the activation of caspase-9, rather than inhibition of P-gp. On the other hand, at the same experimental conditions, Sch B did not enhance DOX-induced apoptosis of adult rat cardiomyocytes and human fibroblasts.

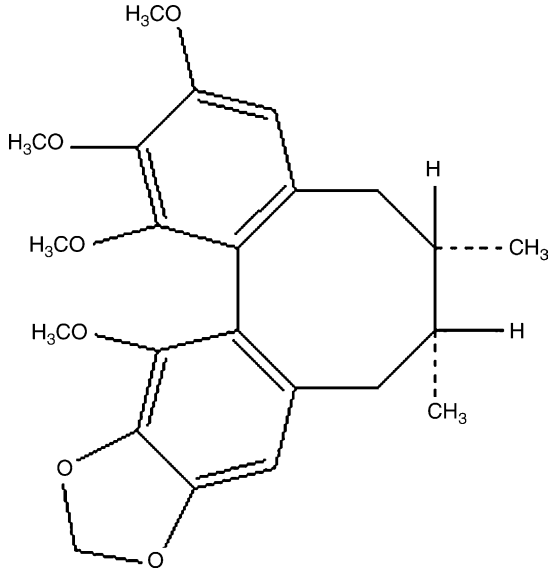

Fig. 1 – The structure of Schisandrin B.

2. Materials and methods

2.1. Reagents

DOX and rhodamin123 (Sigma, St. Louis, MO, USA); Sch B (the National Institute for the Control of Pharmaceutical and Biological Products); RPMI 1640, fetal calf serum, and 0.25% trypsin (GibcoBRL, Grand Island, NY, USA); Trizol reagent, RT-PCR kit (Promega, Madison, WI, USA); R-PE-conjugated mouse anti-human P-gp and MRP1 monoclonal antibody (BD PharMingen, San Diego, CA, USA); All other chemicals were of the highest purity available.

2.2. Cell lines and culture conditions

Primary human fibroblasts were isolated from surgically resected foreskin using a institutionally approved protocol. SMMC7721 and MCF-7 cells were maintained in RPMI-1640 containing 10% fetal calf serum and 300 mg/l glutamine (GibcoBRL, Grand Island, NY, USA), and fibroblasts were maintained in DMEM containing 10% fetal calf serum and 300 mg/l glutamine (GibcoBRL, Grand Island, NY, USA), supplemented with 10% fetal bovine serum. Primary rat cardiomyocytes were kindly provided by Dr. Wang J. (Sir Shao Rou Rou's Hospital, Zhejiang University Medical School) and cultured in DMEM containing 10% fetal calf serum. Cells were grown in a humidified CO_2 incubator at 37 °C, and subcultured with 0.25% trypsin–0.02% EDTA.

2.3. Cell viability assay

Cells were seeded into 96-well plates at a density of 5×10^3/well. For the cell viability assay, cells were incubated with Sch B for 2 days, followed by a MTT assay as described [17,18]. Data were collected by reading at 570 nm with a model ELX800 Micro Plate Reader (Bio-Tek Instruments Inc., Highland Park, USA). The percentage of cell survival was calculated by the following formula: percentage of cell survival = (mean absorbance in test wells)/(mean absorbance in control wells) × 100.

2.4. Apoptosis assays

Apoptotic rates were analyzed by flow cytometry using Annexin V-fluorescein isothiocyanate (FITC)/propidium iodide (PI) kit (Sigma, St. Louis, MO, USA), in which Annexin V bound to the exposed phosphatidylserine on the plasma membrane of the apoptotic cells. Staining was performed

according to the manufacturer's instructions, and flow cytometry was conducted on a FACS Caliber (Becton Dickinson, Mountain View, CA). Statistical analysis was performed using WinMDI software version 2.8. The percentage of the early apoptosis was calculated by the dimension of Annexin V positive but PI negative, while the percentage of the late apoptosis plus necrosis was calculated by the dimension of Annexin V positive and PI positive.

Alternatively, the apoptotic cells were determined by propidium iodide staining as described previously [19]. Briefly, 1×10^6 cells were harvested and washed in PBS, then fixed in 75% ethanol for 24 h at 4 °C. After three-time washes with ice-cold PBS, cells were resuspended in 1 ml of PBS solution with 40 μg of propidium iodide (Sigma, St. Louis, MO, USA) and 100 μg of RNase A (Sigma, St. Louis, MO, USA) for 30 min at 37 °C. Samples were then analyzed for their DNA content by a FACS Caliber. The Sub-G1 population represented the apoptotic cells [19].

2.5. Caspase inhibition assay

The Caspase inhibitor zVAD-FMK and its control zFA-FMK were purchased from R&D Systems Products (Minneapolis, MN, USA) and dissolved in DMSO at a stock concentration of 10 mM. Cells were seeded in six-well plate and treated with DOX, Sch B, or the two drug combined, in the presence or absence of zVAD-FMK (final concentration 50 μM) or zFA-FMK (final concentration 20 μM) for 48 h in a humidified CO_2 incubator at 37 °C. The apoptotic cells were determined by propidium iodide staining as described above.

2.6. DOX uptake and efflux assay

For determination of DOX accumulation and retention, cells were seeded in six-well plates at a density of 1×10^6/well. Cells were incubated with 5 μM DOX with or without 50 μM Sch B in the dark at 37 °C in a humidified CO_2 incubator for an appropriate time interval. Then, cells were trypsinized from the subconfluent monolayer of cells, washed twice with ice-cold PBS, and immediately measured for the intracellular DOX using a FACS Caliber with a 488 nm argon laser for excitation. The red fluorescence of DOX was measured by a 575 nm band-pass filter. In the drug retention assay, cells were incubated with 5 μM DOX in the dark at 37 °C in 5% CO_2 for 60 min. Then cells were trypsinized from the subconfluent monolayer of cells, and the cell pellet was washed twice with ice-cold PBS, resuspended in Hanks solution without phenol red containing 50 μM Sch B or not for 30, 60, 90, and 120 min, and immediately measured for the intracellular DOX using a FACS Caliber at excitation wavelength of 488 nm and emission wavelength of 575 nm [20].

2.7. Quantitative real-time PCR of MDR1 mRNA

MDR1 mRNA was analyzed by quantitative real-time RT-PCR. MDR1 mRNA positive control was extracted from MCF-7/DOX cells, a MDR cell line with over-expression of P-gp. Cells were seeded on 24-well plates at a density of 0.5×10^5/well in the presence of DOX for an appropriate time interval, and collected for total RNA extraction. Total RNA was isolated from MCF-7/DOX cells by a TRIzol reagent according to the manufacturer's instruction. The quality of the total RNA was confirmed by the integrity of 28S and 18S rRNA. The first strand cDNA was synthesized from extracted RNA using an Oligo dT as primer.

Real time PCR reaction was carried out in 50 μl containing the cDNA, primers, fluorescent probe, dNTPs, and Taq enzyme, and performed in the ABI-prism 7700 Sequence Detector™ (PE Applied Biosystems, Foster City, CA, USA). In brief, *MDR1* forward primer 5′-AGAAAGCGAAGCAGTGGTTCA-3′ and *MDR1* reverse primer 5′-CGAACTGTAGACAAACGATGAGCTA-3′ amplified a 90-bp fragment from the *MDR1* cDNA that was detected by the FAM-labeled TaqMan probe 5′-TGGTCCGACCTTTTCTGGCCTTATCCA-3′ [21]. The reaction was performed in triplicate for each RT product. Samples were heated for 2 min at 50 °C and 10 min at 95 °C, followed by 40 cycles of amplification for 15 s at 95 °C and 1 min at 60 °C. The fluorescent signal was determined using Sequence Detector™ software (PE Applied Biosystems, Foster City, CA, USA), giving the threshold cycle number (C_T) at which PCR amplification reached a significant threshold. Then the C_T value is defined as the difference in C_T value for the *MDR1* and GAPDH mRNA, the internal standard, and the relative *MDR1* mRNA expression level was presented as $2^{-\Delta C_T}$.

2.8. RT-PCR of MRP1 mRNA

MRP1 mRNA positive control was extracted from HL60/DOX, a MDR cell line with overexpression of MRP1. The PCR primers were 5-ttc cag cct tcc ttc ctg gg-3 (forward) and 5-ttg cgc tca gga gga gca at-3 (reverse) for β-actin, and 5-ggt gct tcc cac gga gg-3 (forward) and 5-tca acc aca aaa ctg cag cc-3 (reverse) for *mrp1*. Amplification was performed in a DNA thermal cycler (Perkin-Elmer, CA, USA) according to the following protocol: (a) for *mrp1,* initial denaturation for 5 min at 95 °C; 35 cycles of denaturation for 15 s at 95 °C, primer annealing for 15 s at 60 °C, polymerization for 15 s at 72 °C, and final extension for 5 min at 72 °C; (b) for β-actin, initial denaturation for 5 min at 95 °C followed by 35 cycles of denaturation for 15 s at 95 °C, primer annealing for 15 s at 60 °C, polymerization for 15 s at 72 °C; and final extension for 5 min at 72 °C. PCR products were separated on ethidium bromide-stained 1.5% agarose gels. Expected RT-PCR product sizes were 182 bp for *mrp1* and 250 bp for β-actin.

2.9. FACS analysis of P-gp

For determination of P-gp, cells were labeled with R-PE-conjugated mouse anti-human P-gp monoclonal antibody (BD PharMingen, San Diego, CA, USA) according to the manufacture's instruction. The fluorescence intensities of the gated cell populations were measured with a FACS Caliber flow cytometer and analyzed with CELL Quest software (Becton Dickinson, San Diego, CA, USA). Appropriate R-PE-conjugated IgG isotype controls were used for correction of nonspecific labeling.

2.10. Western Blot

Cells (1×10^6/well) were incubated in the presence or absence of drugs for an appropriate time interval. Cells were then lysed

in a sample buffer containing 625 mM Tris–HCl (pH 6.8), 10% SDS, 25% glycerol, 5% β-mercaptoethanol, and 0.015% bromphenol blue, followed by sonication and heat denaturation. The protein (40 μg) was applied to a 12% SDS-polyacrylamide gel, transferred to a nitrocellulose membrane, and then detected by the proper primary and secondary antibodies before visualization by chemiluminescence (Chemiluminescence Kit, Pierce, Rockford, IL). Visualization was performed with a Molecular Imager FX (Bio-Rad Laboratories, CA, USA) using Kodak ID imaging densitometry analysis software on a Macintosh personal computer. The antibodies used are rabbit polyclonal anti-human caspase-3 and mouse monoclonal anti-human PARP (Santa Cruz Biotechnology, CA, USA), mouse monoclonal anti-human caspase-8 and mouse monoclonal anti-human caspase-9 (R&D Systems, Minneapolis, MN, USA), rabbit anti-actin IgG (Biomedical Technologies Inc., Stoughton, MA, USA), and the secondary antibody (HRP-conjugated anti-rabbit IgG; HRP-conjugated anti-mouse IgG, Santa Cruz Biotechnology, CA, USA)

2.11. Detection of mitochondrial membrane potential ($\Delta\Psi_m$)

Loss of mitochondrial membrane potential was assessed by flow cytometry, using a fluorescent indicator Rhodanmin123 (Rh123, Sigma, St. Louis, MO, USA), as described [22–24]. Briefly, cells were treated with DOX in the presence or absence of Sch B for an appropriate interval. Then, Rh123 working solution was added to the culture to the final concentration of 2 μg/ml and then incubated in the dark at 37 °C for 30 min. Cells were then washed with PBS and detected immediately for the fluorescence of Rh123 using a FACS Caliber, at excitation wavelength of 488 nm and emission wavelength of 525 nm.

2.12. Statistical analysis

Data were expressed as the mean ± S.D., and analyzed by the Student's *t*-test. *P*-values below 0.05 were regarded as statistically significant.

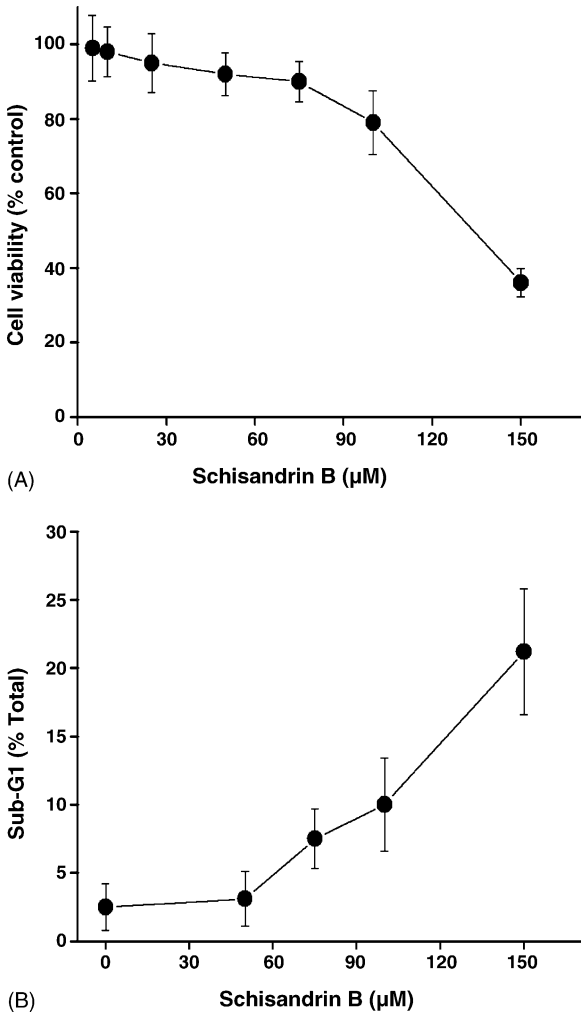

Fig. 2 – Effects of Sch B on proliferation and apoptosis of SMMC7721 cells. Cells were incubated with Sch B for 2 days and subjected for a MTT assay to measure the proliferation or FACS analysis to determine the Sub-G1 cells as described in Section 2. Data were means ± S.D. of three independent experiments.

3. Results

3.1. Sch B enhances DOX-induced apoptosis of cancer cells

In order to set Sch B at concentrations which is nontoxic to cells but could enhance DOX-induced apoptosis, we assayed the cytotoxicities of Sch B at concentrations ranging from 0 to 150 μM. Fig. 2 showed that Sch B at concentrations below 50 μM neither significantly inhibited the growth of SMMC7721 using a MTT assay, nor significantly increased the Sub-G1 (apoptotic) percentage as assayed by a FACS analysis. Therefore, unless otherwise stated, Sch B at 50 μM was used for the subsequent studies.

To test if Sch B was able to enhance DOX-induced apoptosis, we incubated SMMC7721 cells with 1 μM DOX in the presence or absence of Sch B. As shown in Fig. 3, the early and later apoptotic cells constituted 5.1 ± 2.8 and 15.5 ± 4.3%, respectively, when the cells were treated with DOX alone, whereas they constituted 12.2 ± 1.1 and 27.0 ± 6.7, respectively, when the cells were treated with DOX and Sch B combined. Since Sch B alone did not induce apoptosis, it is obvious that Sch B is able to augment the potency of DOX.

The Sch B-enhanced DOX-induced apoptosis was also observed for MCF-7, a human breast cancer cell line (Fig. 4A), when MCF-7 was treated with 1 μM DOX alone, apoptotic cells only accounted for 7.15 ± 1.56%, whereas they accounted for 16.63 ± 1.43%, when cells were treated with DOX and Sch B combined. Fig. 4B showed that Sch B at concentrations below 50 μM did not significantly inhibit the growth of MCF-7.

3.2. Sch B does not enhance DOX-induced apoptosis of normal cells

To test if Sch B can also enhance DOX-induced apoptosis in normal cells, we treated rat cardiomyocytes or human fibroblast cells with DOX in the presence or absence of Sch

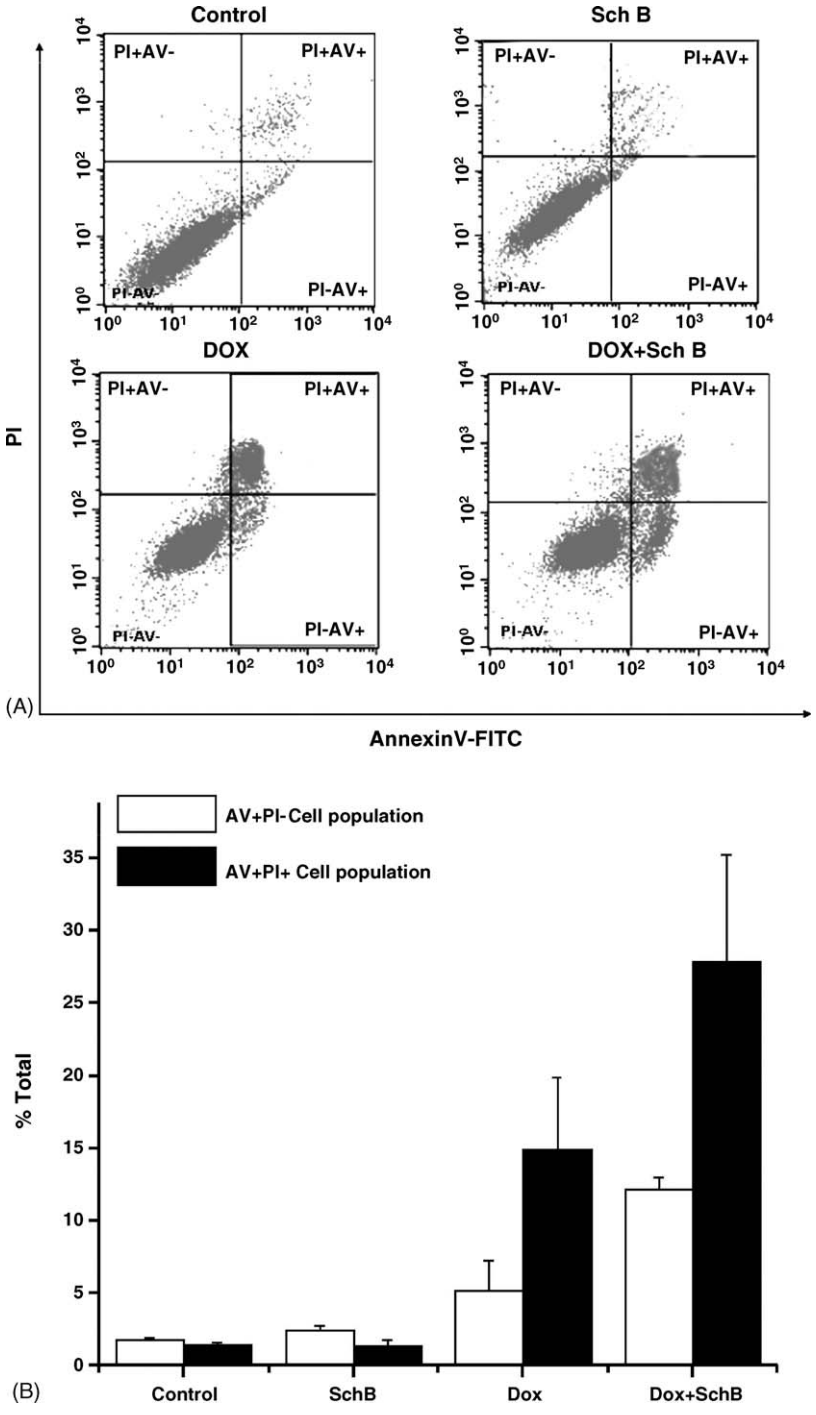

Fig. 3 – Effect of Sch B on the apoptosis of SMMC7721 induced by DOX. Cells were incubated with DOX in the presence or absence of Sch B for 2 days and assayed for apoptosis as described in Section 2. Early Apoptotic cells are Annexin V positive but PI negative; late apoptotic and necrotic cells are Annexin V and PI positive; (A) control, 0.1% DMSO; Sch B, 50 μM; DOX, 1 μM; DOX 1 μM + Sch B 50 μM. (B) Summary of (A). Data are mean ± S.D. of four assays.

B, using a protocol exactly the same as in treating SMMC7721. As shown in Fig. 5A and B, the apoptotic rates induced by DOX alone or combined constituted 7.8 ± 2.1 and $8.82 \pm 1.03\%$, respectively, indicating that Sch B did not enhance the apoptosis of rat cardiomyocytes induced by DOX. Similar results were observed when human fibroblasts were treated with DOX in the presence or absence of Sch B (Fig. 5C).

3.3. *Sch B-enhanced apoptosis is irrelevant with the altered drug transport*

We recently demonstrated that Sch B was a relatively potent inhibitor of P-gp [16]. Therefore, it is possible that the Sch B-enhanced DOX-induced apoptosis is caused by its action on P-gp. To test this possibility, we determined

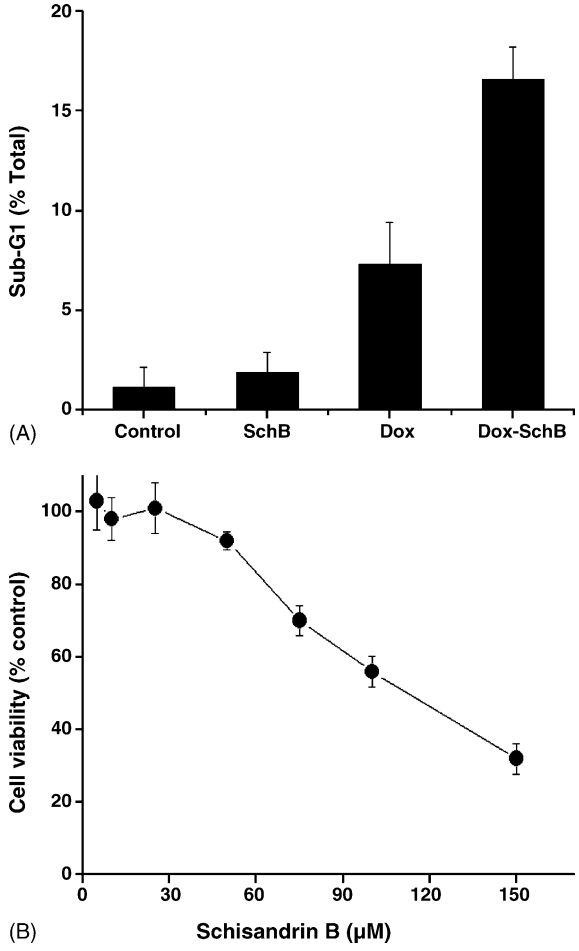

Fig. 4 – (A) Effects of Sch B on enhancing apoptosis of MCF-7 cells induced by DOX. Cells were treated with DOX (1 μM) in the presence or absence of Sch B for 48 h, stained with propidium iodide, and measured for Sub-G1 (apoptotic cell percentage) using a FACS Caliber as described in Section 2. Data are mean ± S.D. of two independent experiments. (B) Inhibition of MCF-7 proliferation by Sch B. Cells were incubated with Sch B for 2 days and subjected for a MTT assay to measure the proliferation as described in Section 2. Data are mean ± S.D. of three independent experiments.

the expression of P-gp and the intracellular DOX accumulation.

Firstly, we determined the expression of MDR1 mRNA in SMMC7721 cells treated with DOX for different time intervals using quantitative real-time RT-PCR. MCF-7/DOX, a breast cancer cell line with overexpression of P-gp, was used as the positive control [16]. Although MDR1 mRNA was detected after exposure to DOX (Fig. 6A), it only constituted less than 0.1% of the positive control. The expression of MDR1 mRNA in SMMC7721 cells was comparable between groups of different times of DOX exposure. To test if P-gp is expressed in SMMC7721 during exposure to DOX, we determined P-gp in those cells by FACS analysis. The results demonstrated that expression of P-gp, if any, is negligible in the cells treated with DOX (Fig. 6B). The results were agreeable with the previous reports [25] that low doses of DOX could slightly increase the mdr1 mRNA but not the protein expression. Therefore, Sch B enhanced DOX-induced apoptosis is unlikely via its action on P-gp, because the latter is not expressed.

We next checked the expression of MRP1 mRNA in SMMC7721 cells treated with DOX for different times. HL60/DOX was used as the positive control. As shown in Fig. 6C, except for the positive control, MRP1 mRNA was not detected in SMMC7721 cells treated with DOX in the indicated exposure time, proving that the Sch B enhanced DOX potency is not a consequence of its inhibition of MRP1.

To test if Sch B-enhanced DOX potency is not a result of its inhibition of any other or undefined drug-transporters which may recognize DOX as a substrate, we examined the effects of Sch B on DOX accumulation in SMMC7721 cells. SMMC7721 cells were exposed to 5 μM DOX in the presence or absence of Sch B (50 μM), and intracellular DOX was determined by flow cytometry at the indicated times. The intracellular DOX in the presence or absence of Sch B was comparable without a significant difference (Fig. 6D). Likewise, there was no significant difference of DOX efflux between the two groups (Fig. 6E). Similar results were obtained when MCF-7 was assayed (data not shown). These data indicated that Sch B-enhanced DOX-induced apoptosis was not a result of its action on any DOX-efflux pumps.

Using confocal microscopic technologies, we observed the intracellular distribution of DOX in SMMC7721 cells in the presence or absence of Sch B. The results showed that Sch B did not affect the intracellular distribution of DOX (data not shown).

3.4. *Sch B-enhanced apoptosis is caspase-dependent*

Since Sch B-enhanced apoptosis in SMMC7721 is irrelevant to drug-transporters, we tested if this enhancement is through mechanisms involving apoptosis pathways. zVAD-FMK, a general caspase inhibitor, was applied to determine whether the apoptosis of SMMC7721 treated with a mixture of DOX and Sch B is caspase dependent or independent. The results showed that zVAD-FMK not only blocked the apoptosis induced by DOX alone or combined treatment, but also abolished the difference ($P > 0.05$) in the apoptotic rate between the two groups (Fig. 7), indicating Sch B enhanced apoptosis is caspase dependent. Similar results were obtained when MCF-7 was assayed (data not shown).

Then we further checked if the caspase-3, the major effector of caspase, and PARP, the main substrate of caspases, were involved. Activation of caspase-3 was assessed by the decreased amount of pro-caspase-3 based on Western blot analysis [26]. Sch B alone resulted in no significant change of pro-caspase-3, as compared with the control. DOX and Sch B combined treatment caused a pronounced reduction of pro-caspase-3, as compared with DOX alone, indicating the enhanced cleavage of the pro-caspase-3 to its active form (Fig. 8). Correspondingly, the cleavage of PARP (85 kDa fragment) was the most pronounced by the DOX-Sch B-combined treatment (Fig. 8), agreeable with the amount change of pro-caspase-3.

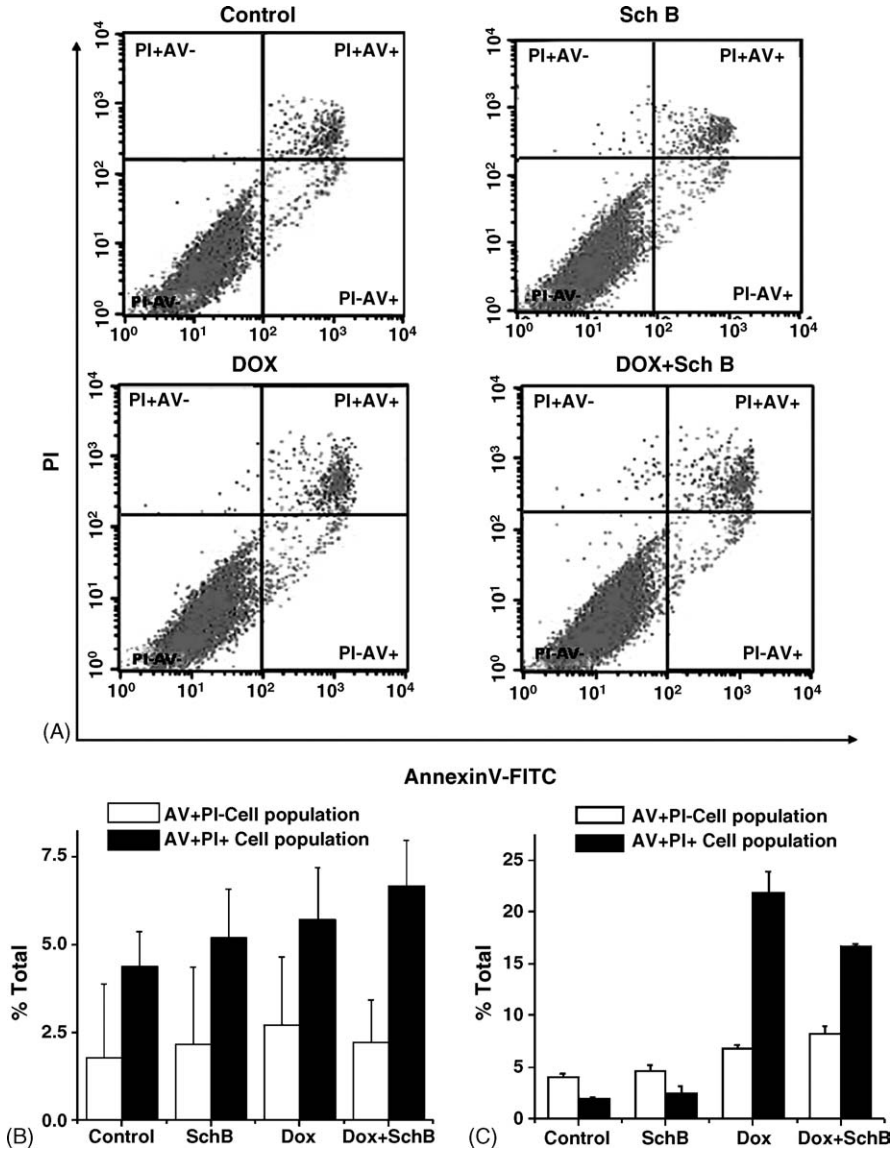

Fig. 5 – Effects of Sch B on DOX-induced apoptosis of normal cells. Adult rat cardiomyocytes (A and B) or human fibroblasts (C) treated with DOX (1 μM) alone or DOX (1 μM) and Sch B (50 μM) combined and subjected for a apoptosis analysis as described in Section 2. Early Apoptotic cells are Annexin V positive but PI negative; late apoptotic and necrotic cells are Annexin-V and PI positive. Data are mean ± S.D. of four independent experiments.

3.5. *SchB enhances apoptosis via caspase-9 rather than caspase-8*

Two distinct apoptotic pathways, the death receptor pathway which activates pro-caspase-8, and mitochondiral pathway which activates pro-caspase-9, were associated with DOX-induced apoptosis. As shown in Fig. 9, Sch B alone activated neither pro-caspase-9 nor pro-capase-8 in SMMC7721 cells. The activation of caspase-8 was comparable between DOX alone and combined treatment (Fig. 9). On the other hand, Sch B and DOX combined treatment caused a cleavage of pro-caspase-9 to its active forms (37 and 29 kDa), significantly more than DOX alone (Fig. 9). Similar data were obtained when MCF-7 was treated the same way as SMMC7721 (data not shown). These results indicated that Sch B enhanced DOX-induced apoptosis most likely via mitochondrial pathway.

Since caspase-9 activation is mainly via the mitochondrial pathway, and since the loss of $\Delta\Psi_m$ is an event in the mitochondria apoptotic pathway earlier than caspase-9 activation, we tested if combined treatment also caused the loss of the mitochondrial membrane potential. Since depolarization of $\Delta\Psi_m$ can be represented by the reduced Rh123 accumulation in mitochondria[22], we used this fluorescent indicator to estimate the effects of DOX and Sch B on the loss of the membrane potential of mitochondria. As shown in Fig. 10, after exposure to 1 μM DOX in the presence of 50 μM Sch B for 48 h, cells exhibited much lower Rh123 staining (270.08 ± 3.93) than control's 408.46 ± 5.22 ($P < 0.01$), although DOX alone reduced Rh123 staining mildly (360.55 ± 3.65).

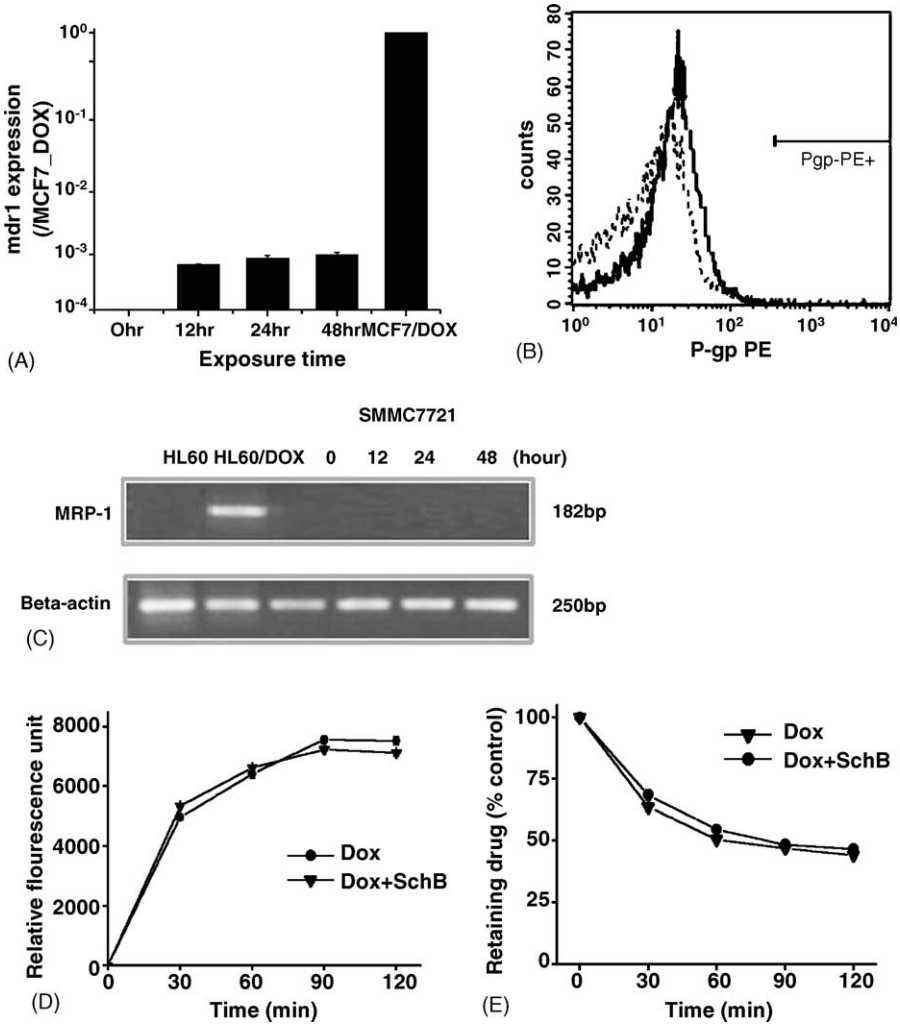

Fig. 6 – Induction of P-gp and MRP1 in SMMC7721 by DOX. Cells were treated with DOX for different times and collected for measurement of P-gp and MRP1 expression. (A) Real-time PCR determination of MDR1 mRNA as described in Section 2. Data are mean ± S.D. of three independent experiments. (B) P-gp was labeled with an R-PE-conjugated mouse anti-human P-gp monoclonal antibody and measured with a FACS Caliber. Dotted line, isotype control; solid line, R-PE-conjugated mouse anti-human P-gp. (C) Detection of MRP1 mRNA by a RT-PCR assay, with the β-actin as the internal control. (D) Effect of Sch B on DOX accumulation in SMMC7721 cells. Cells were exposed to 5 μM DOX with or without Sch B (50 μM) for various times at 37 °C and then measured for intracellular DOX. Data are mean ± S.D. of triplicate determinations. (E) Effect of Sch B on the efflux of DOX in SMMC7721 cells. Cells were exposed to 5 μM DOX for 1 h at 37 °C and then washed with cold PBS, and resuspended in Hank's solution with or without Sch B (50 μM) and incubated for various times at 37 °C. The fluorescent intensity at start of efflux was arbitrarily taken as 100%. Data are mean ± S.D. of triplicate determinations.

There were no significant differences between Sch B alone and control.

3.6. *Sch B-enhanced DOX-induced apoptosis is irrelevant to ROS*

It is recently reported that DOX-induced apoptosis of cancer cells and cardiomyocytes through different apoptotic signaling pathways, while the former was mainly p53 dependent, the latter was mediated by ROS [30]. In this study, we found that Sch B was able to increase the potency of DOX against SMMC7721 and MCF-7 cells but not primary rat cardiomyocytes and primary human fibroblasts. We try to know if Sch B-enhanced apoptosis in cancer cells was associated with DOX's capacity to generate ROS. SMMC7721 cells were treated with DOX, mitoxantrone (an anthracycloquinone that generates much less ROS than DOX) [1], or vincristine (a non-ROS generator) [27] in the presence or absence of Sch B. The results demonstrated that Sch B indiscriminately enhanced the potency of the three drugs (Fig. 11), indicating that apoptotic enhancement by Sch B was irrelevant to the latter's capacity to generate ROS.

4. Discussion

We recently demonstrated that Sch B could reverse cancer MDR via inhibiting P-gp [16]. This finding prompts us to

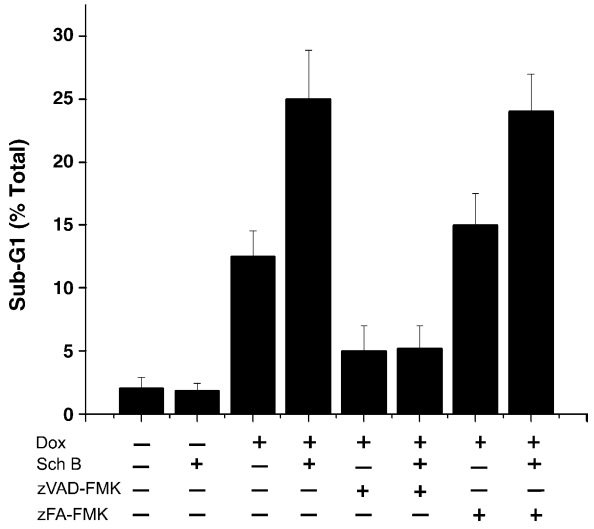

Fig. 7 – Inhibition of apoptosis of SMMC7721 by the caspase inhibitor zVAD-FMK. SMMC7721 cells were incubated with a mixture of 1 μM DOX and 50 μM Sch B with or without zVAD-FMK or zFA-FMK (the control) for 48 h. Apoptotic rate was determined by PI staining. Values represent the mean ± S.D. of triplicate determinations.

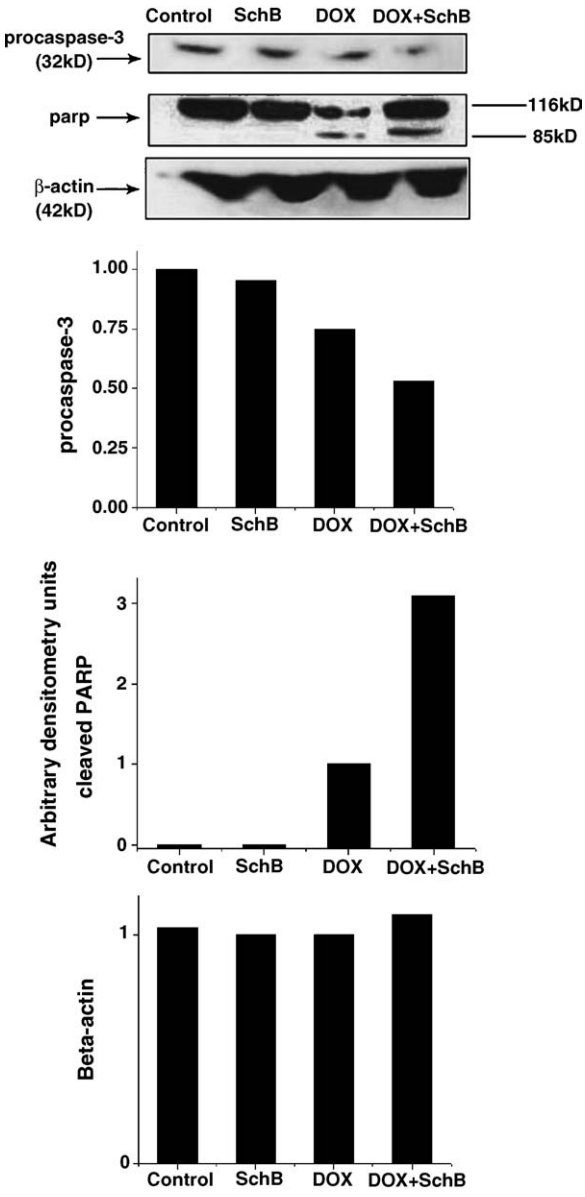

Fig. 8 – Determination of caspase-3 and PARP in SMMC7721 cells treated with DOX in the presence or absence of Sch B by Western Blot. The activation of caspase-3 is reflected by the reduced amount of pro-caspase-3, and the activation of PARP is reflected by the amount of the cleaved 85 kDa PARP. β-Actin served as an internal control. The densities of the bands were quantified by a Kodak ID imaging densitometer, and calibrated by the internal standard β-actin. The data are representative of three separate experiments.

investigate if this compound can also enhance the potency of anthracyclines via other mechanisms rather than P-gp. Choosing anthracyclines for this study is because (1) anthracyclines are a class of very efficacious anti-cancer agents toward a wide spectrum of malignancies and (2) they displayed severe dose-dependent cardiotoxicities once the cumulative doses over 500 mg/m^2 [29]. If Sch B could enhance the anti-cancer efficacies of DOX, it would correspondingly reduce the dose of DOX and its associated toxicities. Indeed, our results indicated that Sch B could enhance DOX-induced apoptosis of cancer cells for about two-fold, but not adult rat cardiomyocytes, suggesting its potential clinical application in the future as an adjuvant.

One of the mechanisms that Sch B enhances DOX-induced apoptosis lies in its capacity to inhibit P-gp and other drug pumps. Since P-gp could efficiently expel the intracellular DOX out of cells, and since Sch B is a relatively potent inhibitor of the former, it is likely that the enhanced DOX-induced apoptosis is in fact the inhibition of P-gp by Sch B, resulting in a significant increase of intracellular DOX and a consequently increased apoptosis. This possibility was ruled out by the evidence that there was no detectable protein of P-gp in SMMC7721 cells. Intracellular drug accumulation and retention assays further demonstrated that it is unlikely that the enhanced apoptosis is a result of its action on other possible drug pumps.

Since Sch B-enhanced apoptosis is not a result of its action on drug pumps, we assumed that it could increase the sensitivity of SMMC7721 cells toward DOX via caspase pathways. Addition of the caspase inhibitor zVAD-FMK blocked DOX-induced apoptosis in the presence or absence of Sch B and abolished the difference of the apoptotic rates between the two groups, proving that the Sch B-enhanced potency of DOX is caspase-dependent. Since DOX could trigger apoptosis in cancer cells via both death-receptor and the mitochondrial pathways, we tried to answer via which apoptotic pathway Sch B enhanced DOX. Our results indicated that whereas Sch B did not enhance the cleavage of pro-caspase-8, it substantially enhanced caspas-9 accompanied with a significant elevation of mitochondrial breakdown, indicating mitochondrial signaled apoptotic pathway is the major mechanism [28].

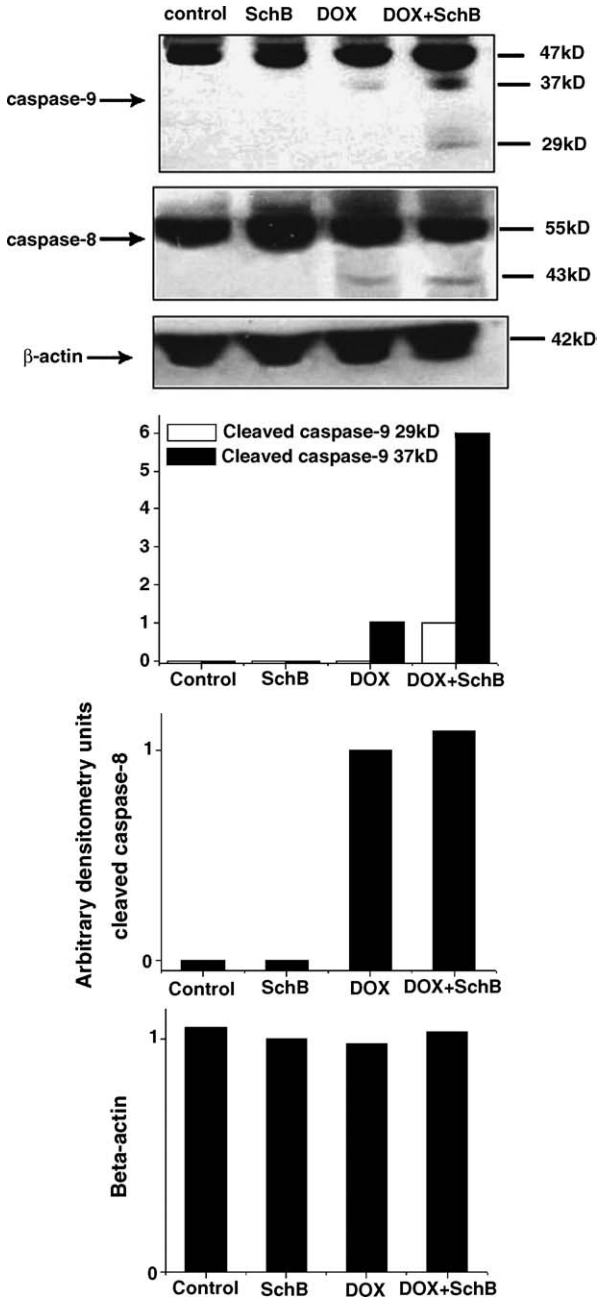

Fig. 9 – Determination of caspase-8 and -9 in SMMC7721 cells treated with DOX in the presence or absence of Sch B by Western Blot. The activation of caspase-9 is reflected by the bands of cleaved 37 and 29 kDa and the activation of caspase-8 is reflected by the band of cleaved 43 kDa. The densities of the bands were quantified by a Kodak ID imaging densitometer, and calibrated by the internal standard β-actin. The data are representative of three separate experiments.

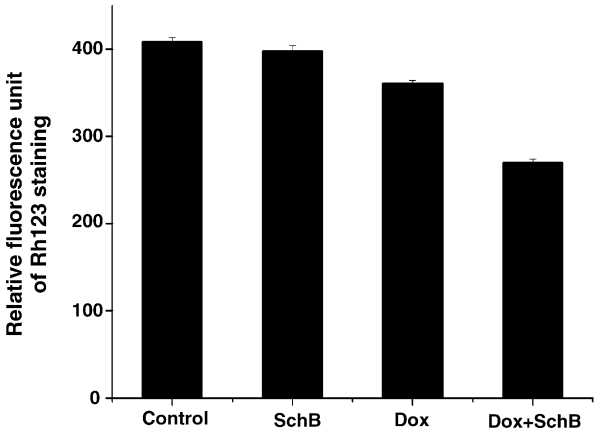

Fig. 10 – Determination of collapse of mitochondrial membrane potential ($\Delta\Psi_m$) in SMMC7721 cells treated with DOX in the presence or absence of Sch B. Data are mean ± S.D. of three independent experiments.

It has been generally accepted that the dilative cardiomyopathy and congestive heart failure caused by DOX are associated with its activities to induce apoptosis of cardiomyocytes. Recently, Wang et al. reported that DOX-induced apoptotic mechanisms in cardiomyocytes and cancer cells were different. While the former is ROS dependent, the latter is ROS independent [30]. In this study, we provided the evidence that Sch B-enhanced potency of anti-cancer drugs against cancer cells is irrelevant with the latter's ability to generate ROS in SMMC7721 cells. Therefore, it is not surprising that while Sch B significantly enhanced the apoptosis of SMMC7721 and MCF-7 induced by DOX, at the same experimental conditions, it did not enhance the apoptosis of primary rat cardiomyocytes induced by this drug.

Besides its activities enhancing the potency of DOX, Sch B has the following advantages as an anti-cancer adjuvant. First of all, Sch B is a potent P-gp inhibitor[16]. Secondly, Sch B is a strong liver protective agent, which is specifically meaningful

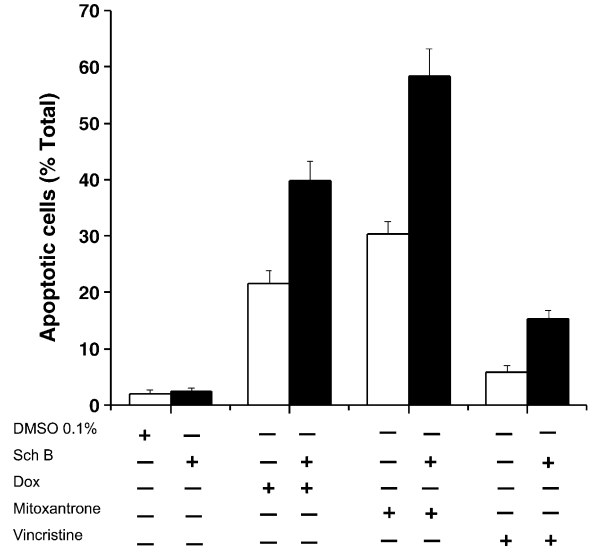

Fig. 11 – Sch B indiscriminately enhances the apoptosis of SMMC7721 induced by DOX, mitoxantrone, or vincristine. Cells were incubated with anti-cancer drugs (DOX, 1 μM, mitoxantrone, 2.5 μM, vincristine, 1 μM) in the presence or absence of Sch B (50 μM) for 2 days and assayed for apoptosis as described in Section 2. Data are mean ± 4 determinations.

for the therapy of hepatic cancers by reducing the hepatic toxicities associated with anti-cancer agents. Thirdly, its activities to improve mitochondrial GSH redox status [31,32] may even mitigate cardiotoxicity induced by repeated administrations of DOX. Lastly, Sch B is of high safety. Sch B is one of the major components present in *Schisandra chinensis*. *S. chinensis* is listed in the Chinese Pharmacopoeia and indexed as a tonic and sedative. Although *S. chinensis* has been widely used as a medication with multiple functions for the last several thousand years in China, the adverse effect of *S. chinensis* associated to the treatment was not reported. The doses of Sch B used to protect the liver caused by carbon tetrachloride were as high as 3 mmol/kg (1200 mg/kg) in mice, indicating virtually nontoxic nature of this compound [33,34]. Further toxic data related to Sch B are refered to the review article [35]. Bearing the multiple functions and high safety, Sch B is of potentials as a candidate adjuvant for cancer therapy.

Acknowledgement

This investigation is supported by Ninbo Innopharma Technologies Ltd., Ninbo, PR China. We thank Dr. Wang J for the generous gift of adult rat cardiomyoctes.

REFERENCES

[1] Minotti G, Menna P, Salvatorelli E, Cairo G, Gianni L. Anthracyclines: molecular advances and pharmacologic developments in antitumor activity and cardiotoxicity. Pharmacol Rev 2004;56:185–229.
[2] Friesen C, Herr I, Krammer PH, Debatin KM. Involvement of the CD95 (APO-1/FAS) receptor/ligand system in drug-induced apoptosis in leukemia cells. Nat Med 1996;2:574–7.
[3] Fulda S, Strauss G, Meyer E, Debatin KM. Functional CD95 ligand and CD95 deathinducing signaling complex in activation-induced cell death and doxorubicin-induced apoptosis in leukemic T cells. Blood 2000;95:301–8.
[4] Lacour S, Hammann A, Wotawa A, Corcos L, Solary E, Dimanche-Boitrel MT. Anti-cancer agents sensitize tumor cells to tumor necrosis factor-related apoptosis-inducing ligand-mediated caspase-8 activation and apoptosis. Cancer Res 2001;61:1645–51.
[5] Clementi ME, Giardina B, Di Stasio E, Mordente A, Misiti F. Doxorubicin-derived metabolites induce release of cytochrome *c* and inhibition of respiration on cardiac isolated mitochondria. Anti-cancer Res 2003;23: 2445–50.
[6] Kalivendi SV, Kotamraju S, Zhao H, Joseph J, Kalyanaraman B. Doxorubicin-induced apoptosis is associated with increased transcription of endothelial nitric-oxide synthase Effect of antiapoptotic antioxidants and calcium. J Biol Chem 2001;276:47266–7.
[7] Kim R. Recent advances in understanding the cell death pathways activated by anti-cancer therapy. Cancer 2005;103:1551–60.
[8] Bian X, Giordano TD, Lin HJ, Solomon G, Castle VP, Opipari Jr AW. Chemotherapy-induced apoptosis of S-type neuroblastoma cells requires caspase-9 and is augmented by CD95/Fas stimulation. J Biol Chem 2004;279:4663–9.
[9] Cai Z, Stancou R, Korner M, Chouaib S. Impairment of Fas-antigen expression in adriamycin-resistant but not TNF-resistant MCF7 tumor cells. Int J Cancer 1996;68:535–46.
[10] Labialle S, Gayet L, Marthinet E, Rigal D, Baggetto LG. Transcriptional regulators of the human multidrug resistance 1 gene: recent views. Biochem Pharmacol 2002;64:943–8.
[11] Scatena CD, Stewart ZA, Mays D, Tang LJ, Keefer CJ, Leach SD, et al. Mitotic phosphorylation of Bcl-2 during normal cell cycle progression and Taxol-induced growth arrest. J Biol Chem 1998;273:30777–84.
[12] Dantzig AH, Shepard RL, Cao J, Law KL, Ehlhardt WJ, Baughman TM, et al. Reversal of P-glycoprotein-mediated multidrug resistance by a potent cyclopropyldibenzosuberane modulator LY335979. Cancer Res 1996;56:4171–9.
[13] Livingston RB. Combined modality therapy of lung cancer. Clin Cancer Res 1997;12:2638–47. Pt 2.
[14] Osklonny MV, Fojo T, Bhalla KN, Kim JS, Trepel JB, Figg WD, et al. The Hsp90 inhibitor geldanamycin selectively sensitizes Bcr-Abl-expressing leukemia cells to cytotoxic chemotherapy. Leukemia 2001;10:1537–43.
[15] Chiu PY, Mak DH, Poon MK, Ko KM. Role of cytochrome P-450 in schisandrin B-induced antioxidant and heat shock responses in mouse liver. Life Sci 2005;13 [Epub ahead of print].
[16] Qiangrong P, Wang T, Lu Q, Hu X. Schisandrin B—a novel inhibitor of P-glycoprotein. Biochem Biophys Res Commun 2005;335:406–11.
[17] Wang T, Chen F, Chen Z, Wu YF, Xu XL, Zheng S, et al. Honokiol induces apoptosis through p53-independent pathway in human colorectal cell line RKO. World J Gastroenterol 2004;10:2205–8.
[18] Chen F, Wang T, Wu YF, Gu Y, Xu XL, Zheng S, et al. Honokiol: a potent chemotherapy candidate for human colorectal carcinoma. World J Gastroenterol 2004;10:3459–63.
[19] Godard T, Deslandes E, Lebailly P, Vigreux C, Poulain L, Sichel F, et al. Comet assay and DNA flow cytometry analysis of staurosporine-induced apoptosis. Cytometry 1999;36:117–22.
[20] Tsang WP, Chau SP, Fung KP, Kong SK, Kwok TT. Modulation of multidrug resistance-associated protein 1 (MRP1) by p53 mutant in Saos-2 cells. Cancer Chemother Pharmacol 2003;51:161–6.
[21] Schiedlmeier B, Kühlcke K, Eckert HG, Baum C, Zeller WJ, Fruehauf S. Quantitative assessment of retroviral gene transfer of the human multidrug resistance 1 gene to human mobilized peripheral blood progenitor cells engrafted in nonobese diabetic/severe combined immunodeficient mice. Blood 2000;95(4):1237–48.
[22] Vander Heiden MG, Chandel NS, Williamson EK, Schumacker PT, Thompson CB. Bcl-xl regulates the membrane potential and volume homeostasis of mitochondria. Cell 1997;91:627–37.
[23] Emaus RK, Grunwald R, Lemasters JJ. Rhodamine 123 as a probe of transmembrane potential in isolated rat-liver mitochondria: spectral and metabolic properties. Biochim Biophys Acta 1986;850(3):436–48.
[24] Chen LB. Fluorescent labeling of mitochondria. Method Cell Biol 1989;9:103–23.
[25] Yague E, Armesilla AL, Harrison G, Elliott J, Sardini A, Higgins CF, et al. P-glycoprotein (MDR1) expression in leukemic cells is regulated at two distinct steps, mRNA stabilization and translational initiation. J Biol Chem 2003;278:10344–52.
[26] Nakahara C, Nakamura K, Yamanaka N, Baba E, Wada M, Matsunaga H, et al. Cyclosporin-A enhances docetaxel-induced apoptosis through inhibition of nuclear factor-kappaB activation in human gastric carcinoma cells. Clin Cancer Res 2003;9:5409–16.
[27] Kamio T, Toki T, Kanezaki R, Sasaki S, Tandai S, Terui K, et al. B-cell-specific transcription factor BACH2 modifies

the cytotoxic effects of anti-cancer drugs. Blood 2003;102(9):3317–22.
[28] Marzo I, Susin SA, Petit PX, Ravaganan L, Brenner C, Larochette N, et al. Caspase disrupt mitochondrial memberane barrier function. FEBS Lett 1998;427:198–202.
[29] Yeung TK, Chakrabarti K, Wilding D, Hopewell JW. Modification of doxorubicin-induced cardiotoxicity: manipulation of the dosage schedule. Hum Exp Toxicol 2002;21:607–14.
[30] Wang S, Konorev EA, Kotamraju S, Joseph J, Kalivendi S, Kalyanaraman B. Doxorubicin induces apoptosis in normal and tumor cells via distinctly different mechanisms. intermediacy of H_2O_2- and p53-dependent pathways. J Biol Chem 2004;279:25535–43.
[31] Chiu PY, Tang MH, Mak DHF, Poon MKT, Ko KM. Hepatoprotective mechanism of schisandrin B: role of mitochondrial glutathione antioxidant status and heat shock proteins. Free Radical Biol Med 2003;35:368–80.
[32] Chiu PY, Ko KM. Schisandrin B protects myocardial ischemia-reperfusion injury partly by inducing Hsp25 and Hsp70 expression in rats. Mol Cell Biochem 2004;266:139–44.
[33] Ip SP, Ko KM. The crucial antioxidant action of schisandrin B in protecting against carbon tetrachloride hepatotoxicity in mice: a comparative study with butylated hydroxytoluene. Biochem Pharmacol 1996;52(11):1687–93.
[34] Ip SP, Poon MK, Che CT, Ng KH, Kong YC, Ko KM. Schisandrin B protects against carbon tetrachloride toxicity by enhancing the mitochondrial glutathione redox status in mouse liver. Free Radical Biol Med 1996;21(5):709–12.
[35] Hancke JL, Burgos RA, Ahumanda F. *Schisandra chinensis* (Turcz.) Bail. Fitoterapia 1999;70:451–71.